Clays and Clay Minerals, Vol. 38, No. 5, 527–536, 1990.

THE NATURE OF CATION-SUBSTITUTION SITES IN PHYLLOSILICATES

WILLIAM F. BLEAM
Soil Science Department, University of Wisconsin, Madison, Wisconsin 53706

Abstract—A fundamental property of electrostatic potentials is their additivity. This study demonstrates that the electrostatic potential of a negatively charged, cation-substituted phyllosilicate layer can be represented as the sum of two potentials. Viewing cation substitution as a defect, one potential is derived from the atoms in a charge-neutral, unsubstituted layer such as pyrophyllite or talc. The "neutral-layer" potential rapidly decays to zero with distance from the layer and is determined primarily by the atoms in the first two atomic planes parallel to the (001) surface, i.e., the basal oxygens and tetrahedral cations. The second component, characterized as a "defect" potential, is a long-range potential derived from cation-substitution. The model used to compute the electrostatic potentials, a two-dimensional Ewald lattice sum, represents the atoms of a single phyllosilicate layer as point charges.

Key Words—Beidellite, Cation-substitution site, Electrostatic potential, Hectorite, Montmorillonite, Vermiculite.

INTRODUCTION

Much of the cation-exchange capacity of smectite and vermiculite is independent of solution pH. This so-called "permanent" surface charge arises from cation substitutions (or less commonly, cation vacancies) in the phyllosilicate layers. These cation-exchange sites influence many important physical properties ranging from swelling and dehydration behavior (cf. McBride, 1989) to the positioning of interlayer cations (Mathieson and Walker, 1954; Shirozu and Bailey, 1966; Odom, 1984; Slade *et al.*, 1985) and the structure of interlayer water (cf. Prost, 1975; Sposito and Prost, 1982). Tetrahedral-sheet substitution of Si^{4+} by Al^{3+} in beidellite and octahedral-sheet substitution of Al^{3+} by Mg^{2+} in montmorillonite or Mg^{2+} by Li^{+} in hectorite are typical examples.

Several prominent clay mineralogists have described the nature of cation-substitution sites in phyllosilicates. Farmer (1978) stated: ". . . the site of substitution is of importance because of its effect on the localization of charge on the surface oxygens." With tetrahedral substitution, according to Farmer (1978), the negative charge resides on the three basal oxygens of the aluminate tetrahedra, whereas the negative charge resides on ten basal oxygens (five on either side of the layer) if octahedral substitution is present. Sposito (1984) employed essentially the same reasoning in a discussion of the relation between substitution-site location and the Lewis basicity of the basal oxygens. The concept of charge localization is also apparent in the statement by Odom (1984): ". . . the tendency for exchangeable cation ordering is not found in octahedrally substituted smectites, since the net charge is more randomly distributed among the surface oxygens." Finally, McBride (1989) described the effect of the substitution site on the hydrogen bonding between inter-layer water molecules and the silicate sheet in this way: ". . . tetrahedral charge is much more localized on fewer surface oxygens than octahedral charge, explaining the stronger H-bonds of adsorbed H_2O on vermiculite."

All of these descriptions of cation-substitution sites have three common elements. First, the negative charge associated with cation substitution is, to some unspecified extent, represented as residing on surface oxygens (i.e., basal oxygens of the tetrahedral sheet). Second, the localization of negative charge on the basal oxygens depends on the location substitution site. Negative charge is characterized as being less localized on the basal oxygens if octahedral substitution is present. Third, no physical mechanism is given to explain how and to what extent negative charge would reside on the basal oxygens.

From the perspective of solid-state chemistry, cation substitution in phyllosilicates does not change the number of valence electrons in the phyllosilicate layer. The number of electrons (i.e., electron-count) is determined by the number of oxygen atoms in the repeat unit (Bleam and Hoffmann, 1988). Cation substitution reduces the nuclear charge at the substitution site by a unit of charge equal to one proton and changes the electronegativity of the atom at the substitution site.

Reducing the nuclear charge by one unit while leaving the electron-count unchanged means that the excess negative charge is actually a positive charge deficit. Because the substituting atom has an electronegativity different from the atom that it replaces, the distribution of electrons near the substitution site will also be perturbed. Some fraction of the excess negative charge remains at the substitution site (i.e., the position occupied by the substituting cation), and the remainder resides on neighboring atoms (both cations and oxygen atoms).

Bleam and Hoffmann (1988) examined the relation between orbital interactions in cation-substituted phyllosilicates and the distribution of charge. Aluminum,

like silicon, has significant capacity to form chemical bonds with oxygen. Bleam and Hoffmann (1988) estimate that if Al^{3+} substitutes for Si^{4+}, ~60% of the excess negative charge resides on the tetrahedral oxygens and only ~35% remains at the tetrahedral cation site. Magnesium atomic orbitals have little tendency to interact with oxygen orbitals to form chemical bonds. As a result, orbital interactions between magnesium and next-nearest-neighbor aluminum atoms becomes the only significant mechanism for redistributing charge, so that if Mg^{2+} replaces Al^{3+}, ~48% of the excess negative charge resides on next-nearest-neighbor aluminum atoms, and ~42% remains at the octahedral cation site (Bleam and Hoffmann, 1988). Kjellander and Marcelja (1985) modeled a mica surface using uncharged oxygen and silicon atoms, assigning a unit negative charge to the specific tetrahedral cation position at which Al^{3+} replaces Si^{4+}. This model captures the essential nature of cation-substitution sites, its only weakness being its complete neglect of charge on atoms other than the excess charge at the substitution site.

The purpose of the present study was to use the charge distributions in cation-substituted phyllosilicates to compute the electrostatic potential at the (001) surface plane. Some calculations used formal charges, whereas others used charges that allowed for charge reduction resulting from chemical bonding. The electrostatic potential was decomposed into two major components using the additive property of potentials. These two components formed the basis of a simple description of the essential properties of the phyllosilicate surface potential.

METHOD

The electrostatic potentials appearing in this paper (*vide infra*) were computed with a two-dimensional Ewald lattice sum. Numerous excellent discussions of this method are found in the scientific literature (e.g., Parry, 1975, 1976; Lee and Choi, 1980; Heyes and van Swol, 1981; Smith, 1983). The focus of the present study was a single, cation-substituted "2:1" phyllosilicate layer. The atoms of this layer and the counterions were represented as point charges possessing translational symmetry in two dimensions.

A lattice sum is the most efficient means of computing potentials if a charge array has translational symmetry. The number of dimensions having translational symmetry determines the dimensionality of the lattice sum; hence, the potentials from a single layer of charge require a two-dimensional sum. The special techniques for taking advantage of translational symmetry are the only characteristics that distinguish this from the more familiar approach of classical electrostatic theory. All the potentials reported in this study were for positions lying outside of and parallel to the planar array of point charges comprising the phyllosilicate layer.

The electrostatic potentials at each point in a rectangular mesh of points parallel to the (001) surface are all that is necessary to prepare a contour map of the electrostatic potential (cf. Foot and Colburn, 1988). Each map in the present paper required ~4200 points and was prepared using the graphics program DI-3000 (version 5.0, Precison Visuals).

Details of the mineral structures used in this study are listed in the Appendix. Chemical bonding results from orbital interactions that have the effect of reducing the atomic charges to some extent. The effect that this has on the electrostatic potential was estimated using extended Hückel, tight-binding calculations of cation-substituted phyllosilicates (Hoffmann and Lipscomb, 1962; Hoffmann, 1963; Whangbo *et al.*, 1979; Bleam and Hoffmann, 1988). The critical point is that without orbital interactions, cation substitution produces a point defect, whereas with orbital interactions, the defect is a localized charge array.

Two idealized dioctahedral structures were used in these calculations to determine the effects of rotation and tilting on the structure of the electrostatic surface potential. Although the tetrahedra in both dioctahedral structures are rotated 10°, one has a corrugated basal surface (produced by 4° tilting of tetrahedra) and the other does not.

Unlike other studies of cation-substituted phyllosilicates (e.g., Baños, 1985; Jenkins and Hartman, 1979, 1980, 1982; Giese, 1979, 1984), tetrahedral and octahedral cations were not assigned statistically averaged charges (Table 1). In other words, all the cation substitutions were ordered even though such ordering is rarely observed in actual diffraction studies (Veitch and Radoslovich, 1963; Bailey, 1975; Weiss *et al.*, 1985). The implications of averaging atomic charges are addressed below.

The electrostatic potential maps all lie 1.98 Å above the centers of the basal oxygens and are parallel to the (001) plane. In the structure having tetrahedral tilting, the distance is measured from the basal oxygens lying on the "ridges" of the corrugations (i.e., those not lying on the mirror plane passing through the M(1) sites). Slade *et al.* (1985) positioned the inter-layer cations 1.98 Å from the basal oxygens in their crystal structure refinement of two-layer hydrates of Na- and Ca-vermiculite. The conclusions derived from these potential maps, however, are not sensitive to the precise position of the map plane relative to the plane of the basal oxygens.

Finally, mineral names have a special meaning to mineralogists and, for this reason, they will not be used when referring to the idealized structures (*vide infra*). Three types of cation substitution will be examined: (1) tetrahedral-sheet substitution of Si^{4+} by Al^{3+} in an idealized pyrophyllite structure to form pseudo-beidellite, (2) octahedral-sheet substitution of Al^{3+} by Mg^{2+} in an idealized pyrophyllite structure to form pseudo-

montmorillonite, and (3) octahedral-sheet substitution of Mg^{2+} by Li^{+} in a talc structure to form pseudo-hectorite. There were no changes in the positions of the atoms of the parent mineral to form the daughter mineral, only changes in the charge assigned to those positions, hence, the prefix pseudo-.

RESULTS

Electrostatic potential surfaces in the (001) surface plane

Figure 1 shows the electrostatic potential in the (001) surface plane 1.98 Å from the surface of pseudo-hectorite. The hexagonal symmetry of the underlying tetrahedral sheet (layer group symmetry: *p6mm*) is readily apparent. Careful inspection, however, reveals distortion of the electrostatic potential from the ideal symmetry of the underlying silicate sheet. Consider now the so-called "defect" potential, found by subtracting (point-by-point) the potential computed for the (001) surface of a neutral phyllosilicate layer from the potential computed for the (001) surface of a cation-substituted phyllosilicate layer. A "defect" potential is shown in Figure 2 in which talc is the neutral mineral and pseudo-hectorite is the substituted mineral. The pseudo-hectorite structure was derived from the talc structure by replacing one of every twelve Mg^{2+} by an Li^{+}, the positions of all other atoms remaining unchanged (cf. Appendix).

The tetrahedra in the silicate sheet of pseudo-montmorillonite are rotated by $\alpha = 11°$. These rotations lower the layer-group symmetry of the tetrahedral sheet to *p3m1*. The electrostatic potential above pseudo-montmorillonite (Figure 3) has a symmetry clearly lower than *p3m1*. The potential has been distorted from the symmetry of tetrahedral sheet. This distortion is not so profound as to render the underlying structure of the silicate sheet unrecognizable. The "defect" potential map (*vide supra*), prepared by subtracting the (001) surface potential of pyrophyllite from the surface potential of pseudo-montmorillonite, is essentially identical to that in Figure 2.

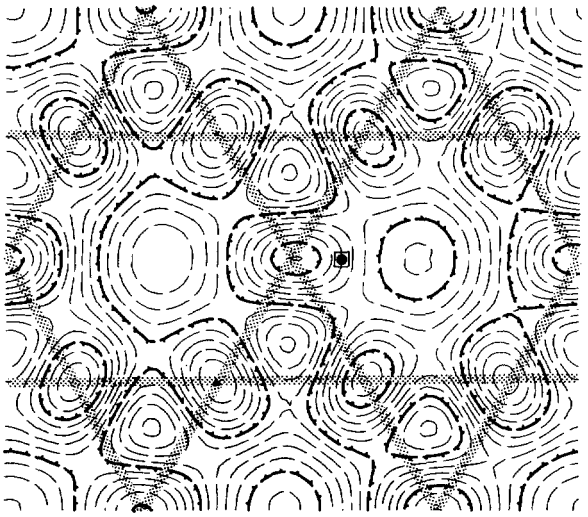

Figure 1. Electrostatic potential map of pseudo-hectorite (001) surface, 1.98 Å above center of basal oxygens. Contour lines are at intervals of 0.05 V. Major contours, identified by tic marks pointing toward lower potentials, are at −1.70, −1.45, and −1.20 V. Shaded lines connect positions of basal oxygens. Substitution site is indicated by square containing a solid circle. Map covers two conventional unit cells, 10.6144 Å by 9.1924 Å.

Cation substitution in both pseudo-hectorite and pseudo-montmorillonite gives rise to a "defect" sur-

Table 1. Atomic charges (in electron units, e) used to compute electrostatic potential maps.

Atom	Hectorite	Montmorillonite	Beidellite
Al	—	2.274,[1] 2.114[2]	2.259,[1] 2.419[3]
H	0.387	0.429	0.419
Li	1.000	—	—
Mg	1.760,[4] 1.720[5]	1.860[6]	—
O_{apical}	−1.460	−1.386	−1.386,[7] −1.506[8]
$O_{hydroxyl}$	−1.220	−1.147,[9] −1.200[10]	−1.123
O_{basal}	−1.217	−1.254	−1.245,[11] −1.365[12]
O'_{basal}[17]	—	—	−1.378,[13] −1.258[14]
Si	2.385	2.489	2.489,[15] 2.429[16]

[1] $Al_{oct}(-OAl_{oct})_2$
[2] $Al_{oct}(-OAl_{oct})(-OMg_{oct})$
[3] $Al_{tet}(-OSi_{tet})_3$
[4] $Mg_{oct}(-OMg_{oct})_3$
[5] $Mg(-OMg_{oct})_2(-OLi_{oct})$
[6] $Mg_{oct}(-OAl_{oct})_2$
[7] $O_{apical}(-Al_{oct})_2(-Si_{tet})$
[8] $O_{apical}(-Al_{oct})_2(-Al_{tet})$
[9] $O_{hydroxyl}(-Al_{oct})_2$
[10] $O_{hydroxyl}(-Al_{oct})(-Mg_{oct})$
[11] $O_{basal}(-Si_{tet})_2$
[12] $O_{basal}(-Al_{tet})(-Si_{tet})$
[13] $O'_{basal}(-Si_{tet})_2$
[14] $O'_{basal}(-Al_{tet})(-Si_{tet})$
[15] $Si_{tet}(-OSi_{tet})_3$
[16] $Si(-OAl_{tet})(-OSi_{tet})_2$

[17] O'_{basal} denotes a basal oxygen lying in the mirror plane passing through the M(1) site and displaced toward the center of the phyllosilicate layer by tilting of the tetrahedra.

https://doi.org/10.1346/CCMN.1990.0380510 Published online by Cambridge University Press

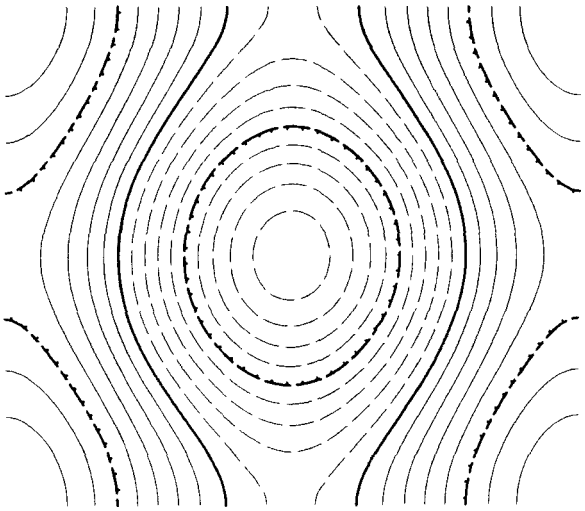

Figure 2. Electrostatic potential map representing difference between pseudo-hectorite (001) surface potential and that of talc (001) surface potential, 1.98 Å above center of basal oxygens. Contour lines are at intervals of 0.05 V. Major contours, identified by tic marks pointing toward lower potentials, are at −0.10, 0.00 and +0.10 V. Potential minimum (above substitution site at center of map) and potential maxima (at the four corners of the map) are −0.194 V and +0.159 V, respectively. Map covers two conventional unit cells, 10.6144 Å by 9.1924 Å.

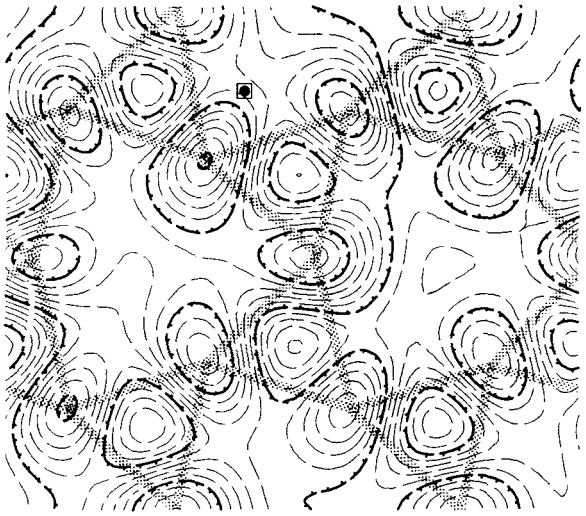

Figure 3. Electrostatic potential map of pseudo-montmorillonite (001) surface, 1.98 Å above center of basal oxygens. Tetrahedra are rotated 11°. Contour lines are at intervals of 0.05 V. Major contours, identified by tic marks pointing toward lower potentials, are at −1.98, −1.73, −1.48 and −1.23 V. Shaded lines connect positions of basal oxygens. Substitution site is indicated by square containing a solid circle. Map covers two conventional unit cells, 10.37455 Å by 8.98463 Å.

face potential, which is smooth compared to the potential that arises from the silicon and oxygen atoms in the first two atomic planes of the phyllosilicate layer. In actuality, the cation substitutions used in this study were not truly point defects. Those oxygen atoms that are nearest neighbors of the substitution site carry a slightly larger negative charge, and cations that are next-nearest neighbors carry a smaller positive charge relative to the other atoms in the structure (Table 1). Strictly speaking, "defect" potentials of the sort appearing in Figure 2 arise from a charge array and not from a point defect.

The electrostatic potential in the (001) plane, 1.98 Å from the basal oxygens and outside of the pseudo-beidellite structure, is shown in Figure 4. The structure of the pseudo-beidellite (and the pyrophyllite from which it was derived) differs from that of pseudo-montmorillonite in that the tetrahedra are tilted 4°. Note that only two potential minima, ascribed to the aluminate basal oxygens, are apparent in the pseudo-beidellite (001) plane and are the result of tilting tetrahedra 4°. The electrostatic potential map clearly illustrates the significance of the tilting distortion. The structure of the underlying tetrahedral sheet is virtually unrecognizable in Figure 4, yet the "defect" potential for pseudo-beidellite is as smooth as the one shown in Figure 2.

Electrostatic potential transects in the (001) surface plane

The potentials plotted along a transect in the (001) plane, passing directly over the substitution sites in pseudo-montmorillonite and pseudo-beidellite, illustrate further the relative magnitudes of the "neutral layer" and "defect" potentials [Figures 5 (upper) and 5 (lower)]. Three curves are present in each illustration. The "neutral" curve is the potential along the transect in the (001) plane 1.98 Å from the basal oxygens of pyrophyllite from which the substituted mineral was derived. The "charged" curve is the potential along the same transect for either pseudo-montmorillonite [Figure 5 (upper)] or pseudo-beidellite [Figure 5 (lower)]. The "defect" potential is simply the "charged" potential minus the "neutral" potential.

The distance between the plane of the counter-ions and the plane passing through the basal oxygens is the same in both illustrations, but the distance between the substitution site and the counter-ion is 4.957 Å in octahedrally substituted pseudo-montmorillonite [Figure 5 (upper)] and 2.465 Å in tetrahedrally substituted pseudo-beidellite [Figure 5 (lower)], a difference of 2.491 Å. The "defect" potential above tetrahedrally substituted phyllosilicates [Figure 5 (lower)] has a barrier height of ~1.5 V separating substitution sites, whereas the electrostatic potential above neutral-layer pyrophyllite has a relief ~0.5 V.

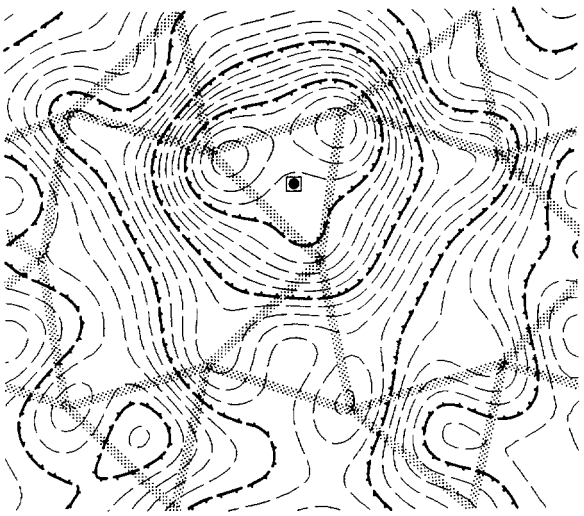

Figure 4. Electrostatic potential map of pseudo-beidellite (001) surface, 1.98 Å above center of basal oxygens. Tetrahedra are rotated 11° and tilted 4°. Contour lines are at intervals of 0.10 V. Major contours, identified by tic marks pointing toward lower potentials, are at −5.0, −4.5, −4.0 and −3.5 V. Shaded lines connect positions of basal oxygens. Substitution site is indicated by square containing a solid circle. Map covers two conventional unit cells, 10.37455 Å by 8.96276 Å.

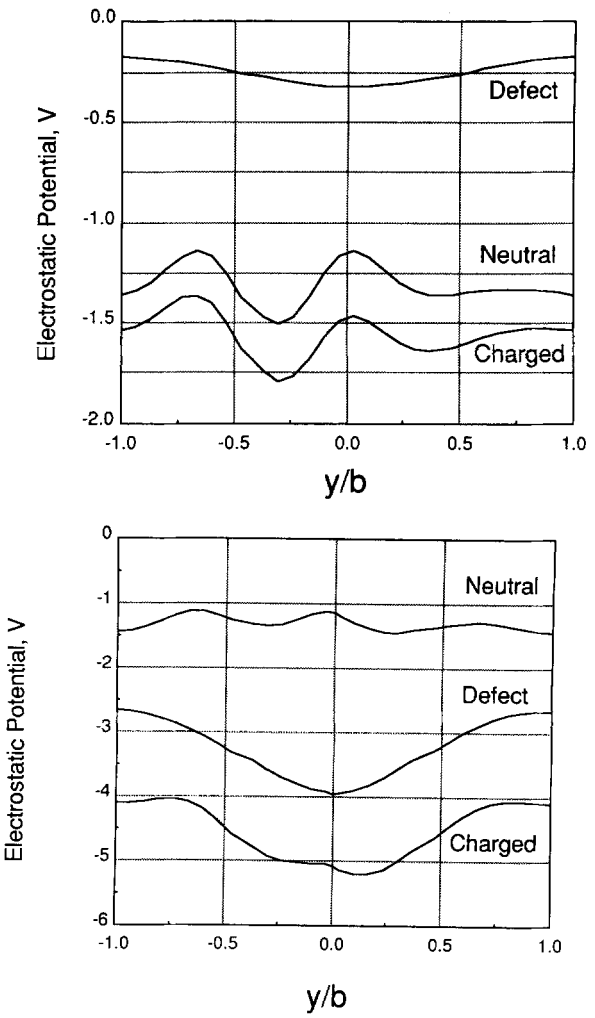

Figure 5. Electrostatic potentials in (001) surface plane above phyllosilicate layers, 1.98 Å above center of basal oxygens: (upper) octahedrally substituted pseudo-montmorillonite and (lower) tetrahedrally substituted pseudo-beidellite. "Charged" labels potentials along transect passing above substituted site of the given phyllosilicate. "Neutral" labels potentials above pyrophyllites, from which the two substituted minerals were derived (see text), along transects appropriate to position of the substitution. "Defect" labels potentials computed by subtracting the "neutral" curve from the "charged" curve for each type of substitution.

Electrostatic potentials normal to the (001) surface plane

The potential measured normal to the (001) plane, outside of cation-substituted phyllosilicates, is the sum of two potentials. One potential arises from the silicon and oxygen atoms in the first two atomic planes of the tetrahedral sheet and is the same for both neutral-layer (e.g., talc and pyrophyllite) and charged-layer minerals (e.g., hectorite, montmorillonite, and beidellite). The second component of the surface electrostatic potential is due to the cation-substitution point defect.

Figure 6 shows the electrostatic potential of a single pseudo-montmorillonite counter-ion as a function of the distance separating the phyllosilicate layer from the plane containing the counter-ions. The z-axis is taken to be normal to the (001) plane with the origin at the octahedral-cation plane (i.e., the plane containing the substitution sites). The curve labeled with open squares was computed by assigning formal charges to all the atoms in the layer, whereas the curve labeled with solid squares employed computed charges (cf. Table 1). Both of these curves approach $-\infty$ as z approaches zero, whereas at large z values, the curve becomes linear and thereby approaches $+\infty$.

These two curves express the self-potential of a positive point charge in a two-dimensional, infinite plane of positive point charges separated by a distance z from a single pseudo-montmorillonite layer. Both the positively charged counter-ions and the negatively charged substitution defect are arranged in a rectangular lattice (layer-lattice symmetry: *p2mm*), with the positive charges lying directly above the negatively charged defects. The linear portion of both pseudo-montmorillonite layer curves, which approaches $+\infty$ at large z, extrapolates to the finite potential, $V(z=0)_{Layer} \approx -4.98$ V. The repeat unit for pseudo-montmorillonite is defined by the lattice vectors: $a = 10.37544$ Å, $b = 8.98463$ Å. Potentials for these two curves are not plotted for $z < 5.0$ Å, because in that range the counter-ions enter

https://doi.org/10.1346/CCMN.1990.0380510 Published online by Cambridge University Press

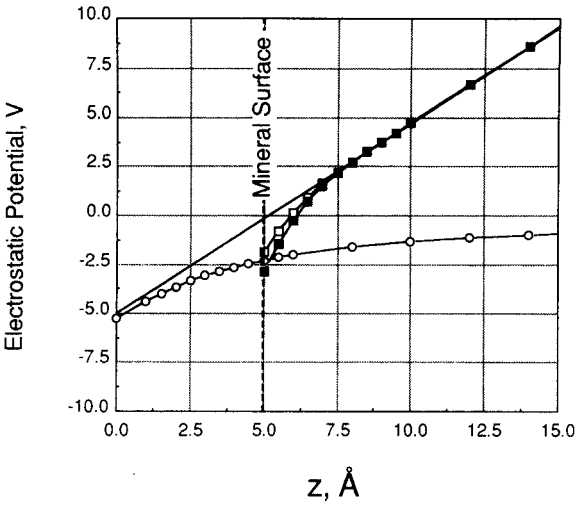

Figure 6. Squares label the electrostatic self-potential of a positive point-charge lying in a rectangular plane-lattice of positive point-charges positioned directly above cation-substitution sites in a single layer of pseudo-montmorillonite. Circles label electrostatic self-potential of a single positive point-charge positioned directly above a negative charge distributed uniformly over a rectangular region. Assigning formal (open squares) and computed (solid squares) charges to atoms in pseudo-montmorillonite yields slightly different curves. Dimensions of rectangular lattice of point-positive charges, dimensions of repeat unit in pseudo-montmorillonite, and dimensions of uniform-rectangular charge distribution are equal: a = 10.37455 Å and b = 8.98463 Å.

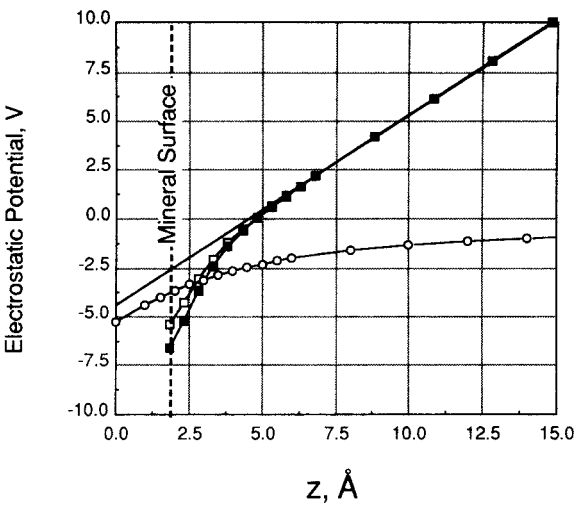

Figure 7. Squares label electrostatic self-potential of a positive point-charge lying in a rectangular plane-lattice of positive point-charges positioned directly above cation-substitution sites in a single layer of pseudo-beidellite. Circles label electrostatic self-potential of a single positive point-charge positioned directly above a negative charge distributed uniformly over a rectangular region. Assigning formal (open squares) and computed (solid squares) charges to atoms in pseudo-beidellite yields slightly different curves. Dimensions of rectangular lattice of point-positive charges, dimensions of repeat unit in pseudo-beidellite, and dimensions of uniform-rectangular charge distribution are equal: a = 10.37455 Å and b = 8.96276 Å.

the layer and the counter-ion self-potentials are no longer physically meaningful.

A third potential curve (labeled with open circles) is also illustrated in Figure 6. The limit of this potential curve as z approaches $+\infty$ is zero. It is finite and negative at z = 0. This curve is the z-dependent self-potential of a single point charge above a uniformly charged planar distribution of equal and opposite charge [Appendix, Eq (A.5)]. Using a circular disk of radius, $R = (ab/\pi)^{1/2}$, or a rectangle of area, $\Omega = ab$, gives nearly the same result. For a rectangular charge distribution having the same dimensions as the pseudo-montmorillonite repeat unit (*vide supra*), $V(z = 0)_{Point} \approx -5.25$ V.

Two curves (open and solid squares), representing the electrostatic potential normal to the pseudo-beidellite layer, are shown in Figure 7. The z-axis is normal to the (001) plane, with the origin taken to be the plane containing the tetrahedral cations, i.e., the plane containing the substitution sites. The curves in Figure 7 are analogous to those in Figure 6. These curves give the self-potential of a counter-ion positioned directly over the substitution site in pseudo-beidellite. The linear portion of this curve extrapolates to a finite potential, $V(z = 0)_{Layer} \approx -4.42$ V. The repeat unit for pseudo-beidellite is defined by the lattice vectors a = 10.37544 Å and b = 8.96276 Å. Potentials do not appear for z < 2.0 Å because for these values the counter-ions enter the layer and the potentials are no longer physically meaningful. The curve labeled with open circles in Figure 7 represents the z-dependent self-potential of a single point charge above a uniformly charged planar distribution of equal and opposite charge. Using a rectangular charge distribution [Appendix, Eq. (A.5)] having the same dimensions as the pseudo-beidellite repeat unit, the limiting potential is: $V(z = 0)_{Point} \approx -5.26$ V.

DISCUSSION

Physical mechanisms for the redistribution of charge

Only two ways exist by which charge can be redistributed in a solid material: (1) induced polarization arising from the electronic polarizability of atoms, and (2) orbital interactions. Electronic polarization of an atom, a displacement of the electron cloud relative to the nucleus induced by the local electric field intensity, causes a charge separation only on the order of the diameter of the atom (cf. Kittel, 1986), i.e., ~2.5 Å for oxygen. Orbital interactions are capable of displacing modest amounts of electron density over slightly larger distances, equivalent to next-nearest neighbor cation–

https://doi.org/10.1346/CCMN.1990.0380510 Published online by Cambridge University Press

cation distances, which in phyllosilicates is ~3.0 Å (Bleam and Hoffmann, 1988).

Electronic polarization of oxygen can lead to significant charge displacement given the magnitude of the electrostatic field intensity attainable within polar inorganic crystals (Bertaut, 1978), the electronic polarizability of oxygen (cf. Kittel, 1986) and the ionic radius of oxygen. Computing the charge displacement by this mechanism is beyond the scope of this study and requires an estimate of the electric field intensity normal to the (001) surface.

Redistribution of charge via orbital interactions reduces ionic charges and thereby decreases the electrostatic potentials within the crystal to about half the magnitude found using formal charges. It has little effect, however, on the potential experienced by a counter-ion located outside the phyllosilicate layer (see Figures 6 and 7).

Implicit in the creation of a cation-substitution defect is the fact that the electron count in the unit cell remains unchanged. This is because the number of occupied electronic states, set by the oxygen atom content of the repeat unit, remains unchanged (Bleam and Hoffmann, 1988). The only change (neglecting for the moment electronic polarization and orbital interactions) is that at the site of the substitution, the core charge of the atom (nuclear charge minus the total number of electrons in the core energy shells) is lowered. Typically, this positive charge deficit is equal to the charge of one proton. Orbital interactions and electronic polarization shift the valence electrons screening the core charges of the atoms within the layer, but they do not cancel the charge.

Components of the electrostatic surface potential

The electrostatic potential maps (Figures 1, 3, and 4) show how the detailed structure of the self-potential includes both short-range and long-range components. The short-range component is determined by the atoms in the first two atomic planes. The long-range interaction of the counter-ion is with the positive-charge deficit. This is more or less the model Kjellander and Marcelja (1985) used in their simulation of the diffuse-double layer. The oxygen and silicon atoms of the silicate sheet in the Kjellander-Marcelja model of (001) plane of mica are neutral and have no effect on the dynamics of the system, except through the "core-repulsion" potential assigned to them. By neglecting the charge on these atoms, the Kjellander-Marcelja model neglects important contributions to the phyllosilicate (001) surface potential.

The intuitive analyses of Low (1962) and Bolt (1979) were correct, in that the charge need not be "smeared out" to give rise to a more or less equipotential surface. Figures 5 (upper), 6, and 7 clearly demonstrate that the long-range component of the electrostatic potential (i.e., the "defect" potential) has already become nearly equipotential, for the extent of substitution used in this study (see Appendix), ≈2.5 Å from the basal oxygens of an octahedrally substituted phyllosilicate (001) surface. At separations exceeding ≈7.5 Å between the plane containing the substitution sites and the plane containing the counter-ions, i.e., about three oxygen diameters, the difference between tetrahedrally and octahedrally substituted systems is negligible. Thus, the potential of an interlayer ion in pseudo-montmorillonite separated from the surface by one water layer (i.e., d(001) ≈ 15 Å) is equivalent to the potential of an interlayer cation in pseudo-beidellite separated from the surface by two water layers (i.e., d(001) ≈ 20 Å).

Of course, the phyllosilicate (001) surface potential is only one factor influencing the structure of the interlayer water and cations. Whereas positioning an interlayer cation directly above a substituted aluminate tetrahedron is clearly not an unstable arrangement, as originally thought by Farmer and Russell (1971), a detailed critical analysis of interlayer models (e.g., Mathieson and Walker, 1954; Shirozu and Bailey, 1966; Prost, 1975; Fripiat *et al.*, 1980; Conard *et al.*, 1984; Slade *et al.*, 1985) must rest on calculations that include two phyllosilicate layers, counter-ions, and water molecules.

Ordered vs. disordered cation substitutions

Jenkins and Hartman (1982) modeled such a system, but they used an approximation that may prejudice certain of their results, i.e., all structural cations in a given (001) surface plane were assigned statistically averaged charges. Statistically averaged charges were also used in the study of expansion energies that led Jenkins and Hartman (1980) to conclude that it took less energy to expand a tetrahedrally substituted phyllosilicate than one that was octahedrally substituted. This conclusion is a direct result of their use of averaged charges.

Two simple examples clarify the meaning of statistically averaged charge. For a beidellite structure having x tetrahedral substitutions per formula unit (i.e., $M_x[Al_2(Si_{4-x}Al_xO_{10})(OH)_2]$), all tetrahedral cations are assigned the same charge: $q_{tet} = [(16 - x)/4]$. All octahedral cations in montmorillonite having x substitutions per formula unit (i.e., $M_x\,[Al_{2-x}Mg_x(Si_4O_{10})(OH)_2]$) are assigned the charge: $q_{oct} = [(6 - x)/2]$.

Jenkins and Hartman (1980) expressed the interaction energy of a counter-ion with a substituted phyllosilicate layer having charge density $\rho = -q/ab$ as:

$$U(z) \approx [-q\rho/z] \quad (1)$$

which makes the self-potential of the counter-ion:

$$V(z) \approx [-\rho/z]. \quad (2)$$

Eqs. (1) and (2) cannot be correct expressions for a two-

https://doi.org/10.1346/CCMN.1990.0380510 Published online by Cambridge University Press

dimensional, infinite layer of charges. The limit as z approaches $+\infty$ should be $+\infty$ (see Fripiat *et al.*, 1977; Watson *et al.*, 1981), whereas the limit as z approaches zero should be a negative but finite value [see Eq. (A.5)]. Eq. (2) fails at both limits.

In the configuration used by Jenkins and Hartman (1980), either all of the charge is in *one* rectangular region ($\rho_{oct} = -q/ab$) at a distance $z_{oct} = l + d$ from the counter-ion (i.e., octahedral substitution) or the charge density is equally spread over *two* rectangular regions ($\rho_{tet,1} = \rho_{tet,2} = -q/2ab$) at distances $z_{tet,1} = l$ and $z_{tet,2} = l + 2d$ (i.e., tetrahedral substitution). In the Jenkins and Hartman (1980) model of tetrahedral substitution, a particular counter-ion can be in close contact with only one of the two regions, the closest approach to the remaining half of the layer charge being $z = 2d$. The counter-ion of an octahedrally substituted phyllosilicate is always found at a lower potential relative to the counter-ion of a tetrahedrally substituted phyllosilicate using the Jenkins and Hartman (1980) charge distribution. Using either Eq. (A.2) or Eq. (A.5), this consequence of using averaged charges can be verified.

In reality, the charge is not averaged over all cations, there being no physical basis for such an averaging. Counter-ions at a given hydration state can always approach a tetrahedral site more closely than an octahedral site and thus attain a more negative electrostatic potential.

Lewis basicity of basal oxygens

Sposito (1984, 1989) discussed the character of the phyllosilicate (001) surface cation-substitution sites in terms of the siloxane cavity, i.e., the 6-fold rings in the tetrahedral sheet. The basal oxygens in the 6-fold ring unquestionably present a geometry suitable for cation coordination, yet crystal structure refinements of hydrated vermiculite (Mathieson and Walker, 1954; Shirozu and Bailey, 1966; Slade *et al.*, 1985) indicate that interlayer cations commonly lie above the substituted tetrahedra. The nature of the electrostatic potential at the (001) surface is probably more important than the geometry of the 6-fold ring in determining the positioning of the interlayer cation.

The Sposito (1984, 1989) model also considers the Lewis base character of the basal oxygens. The bond-strength sum for basal oxygens bridging aluminate and silicate tetrahedra is $\zeta_0 = 1.8$ valence units (Pauling, 1929). The bond strength sum of basal oxygens in octahedrally substituted phyllosilicates does not differ from the bond strength sum for basal oxygens in pyrophyllite and talc because cation substitutions affect only those cation-oxygen bonds within the coordination polyhedra containing the substituting cation. The electrostatic valence principle and valence bond theory (Pauling, 1929; Brown, 1978) predict that the Lewis character of neutral and octahedrally substituted phyllosilicates should be comparable.

Brown (1978) assigned $\sim$0.2 valence units to the O$\cdots$H bond of an oxygen receiving a normal hydrogen bond. The Lewis basicity of basal oxygens ranges from that found in neutral-layer and octahedrally substituted phyllosilicates to that found in tetrahedrally substituted phyllosilicates. The basal-oxygen basicity in the former is so weak that the oxygens cannot effectively receive a hydrogen bond (i.e., $\zeta_0 = 2.0$ valence units), whereas the aluminate oxygens in the latter would rank as good hydrogen bond receptors. Increased Lewis base strength of aluminate oxygens results from the increased electron population in tetrahedral oxygens coordinating aluminum, estimated to be $\sim$12% relative to pyrophyllite or talc (Bleam and Hoffmann, 1988). Electronic polarization (*vida supra*) produces no variation in the Lewis basicity of basal oxygens, because it is no more than a shift in the center of gravity of charge.

Electrostatic field intensity flux

Potentials are additive, allowing a separation of the "charged-layer" potential into "neutral-layer" and "defect" components. The "charged-layer" potential is most easily viewed as a "neutral-layer" potential perturbed by a "defect" potential. The flux of the electrostatic field intensity increases as the distance separating the test charge and the substitution site decreases. The nonuniformity of the flux in the (001) surface is more pronounced at small separations. The relation between the electrostatic field intensity flux and charge separation is expressed in the electrostatic potential maps as a distortion of the "neutral-layer" potential caused by the cation-substitution defect. The distortion of the electrostatic potential is more extreme for tetrahedral substitution than for octahedral substitution. In other words, as the substitution site is approached, the number of electrostatic field lines per unit area increases. What has been described as "localized charge" (Farmer, 1978; Sposito, 1984; Odom, 1984; McBride, 1989) is more correctly termed "increased electrostatic field flux."

Negative potentials in the (001) plane occur not because the layer charge is localized on the basal oxygens, but rather because the surface oxygens producing those potentials are not screened. The notion that cation substitution causes negative charge to reside on the basal oxygens is inaccurate. Consider the difference between the curves due to computed (open squares) and formal (solid squares) charges in Figures 6 and 7. This difference in counter-ion electrostatic self-potentials for these two alternatives for assigning ion charges arises from differences in the charge distribution at the defect. If formal charges are used, the cation-substitution defect consists of a point positive-charge deficit at the sub-

stitution site, the charges on the oxygen atoms remain unchanged in this substitution model. The potential using computed charges (Table 1) represents a substitution model, in which the defect is actually an array of charges consisting of a partial charge at the substitution site, with the remainder assigned to the oxygens immediately surrounding it and the cations next-nearest neighbors to that site. Although the potentials experienced by the atoms within the phyllosilicate layer are substantially different in the two models, the counter-ion potentials are virtually identical.

APPENDIX

Mineral structures

The pseudo-hectorite ($M_x[Mg_{3-x}Li_x(Si_4O_{10})(OH)_2]$, x = 0.25) structure was derived from the refinement of talc by Perdikatsis and Burzlaff (1981). The pseudo-montmorillonite ($M_x \cdot [Al_{2-x}Mg_x(Si_4O_{10})(OH)_2]$, x = 0.25) and pseudo-beidellite ($M_x \cdot [Al_2(Si_{4-x}Al_xO_{10})(OH)_2]$, x = 0.25) structures were derived from the refinement of pyrophyllite by Lee and Guggenheim (1981). Tetrahedral rotation was 11° in both derivations.

The tetrahedra of the silicate sheets have point group symmetry $\bar{4}3m$; the octahedra are flattened and have point group symmetry $\bar{3}m$. Neglecting cation order, the layers themselves have layer group symmetry $c2/m$, whereas the tetrahedral sheets have layer group symmetries $p6mm$, $p3m1$ and $c1m1$ in pseudo-hectorite, pseudo-montmorillonite and pseudo-beidellite, respectively. Important distances in pseudo-hectorite are: d(Si–O) = 1.625 Å; d(X–O) = 2.098 Å; d(O–H) = 0.864 Å (X = Mg, Li). Important distances in pseudo-montmorillonite and pseudo-beidellite are: d(T–O) = 1.618 Å; d(X–O) = 1.912 Å; d(O–H) = 0.864 Å (T = Si, Al; X = Mg, Al).

The tetrahedra are tilted 4°, as found by Lee and Guggenheim (1981), in tetrahedral sheet of pseudo-beidellite. The tetrahedra in pseudo-montmorillonite are not tilted because even in celadonite both octahedral sites are the same size (Bailey, 1975; Weiss *et al.*, 1985).

Electrostatic potential functions

If a charge, −q, is uniformly distributed over a circular disk of radius R, the charge density per unit area is: $\rho = -q/\pi R^2$. The electrostatic potential at a position z above the center of this charge distribution is:

$$V(z) = (\rho/4\pi\epsilon_0)\int_0^{2\pi}\int_0^{R}[r(z^2 + r^2)^{-1/2}]\,dr\,d\theta \quad (A.1)$$

$$V(z) = (\rho/4\pi\epsilon_0)[-2\pi z + 2\pi(z^2 + R^2)^{1/2}] \quad (A.2)$$

$$V(z = 0) = (\rho/4\pi\epsilon_0)[2\pi R] = -q/(2\pi\epsilon_0 R). \quad (A.3)$$

If a charge, −q, is uniformly distributed over a rectangle of dimensions a and b, the charge density per unit area is: $\rho = -q/ab$. The electrostatic potential at a position z above the center of this charge distribution is:

$$V'(z) = (\rho/4\pi\epsilon_0)\int_{-b/2}^{b/2}\int_{-a/2}^{a/2}[x^2 + y^2 + z^2)^{-1/2}]\,dx\,dy. \quad (A.4)$$

Integrating and simplifying using the function $f(z) = (a^2/4 + b^2/4 + z^2)^{1/2}$ yields:

$$\begin{aligned}V'(z) = (\rho/4\pi\epsilon_0)\{&2z\arctan[(-a/2 - b/2 + f(z))/z]\\ &- 2z\arctan[(a/2 - b/2 + f(z))/z]\\ &- 2z\arctan[(-a/2 + b/2 + f(z))/z]\\ &+ 2z\arctan[(a/2 + b/2 + f(z))/z]\\ &- b\ln[-a/2 + f(z)] + b\ln[a/2 + f(z)]\\ &-a\ln[-b/2 + f(z)] + a\ln[b/2 + f(z)]\},\end{aligned} \quad (A.5)$$

and

$$\begin{aligned}V'(z = 0) &= (\rho/4\pi\epsilon_0)\{-b\ln[-a/2 + f(0)] + b\ln[a/2 + f(0)]\\ &\quad -a\ln[-b/2 + f(0)] + a\ln[b/2 + f(0)]\}.\end{aligned} \quad (A.6)$$

The limit as $z \to \infty$ for both Eq. (A.2) and Eq. (A.5) is clearly zero, as expected. These potential functions show that a single point charge in contact with a uniform planar charge distribution is at a finite potential, the exact value of which depends on both the area and the configuration of the uniform planar charge.

REFERENCES

Bailey, S. W. (1975) Cation ordering and pseudosymmetry in layer silicates: *Amer. Mineral.* **60,** 175–187.

Baños, J. O. (1985) Interlayer energy for partial slip and cleavage in muscovite: *Philos. Mag. A* **52,** 145–152.

Bertaut, E. F. (1978) Electrostatic potentials, fields and field gradients: *J. Phys. Chem. Solids* **39,** 97–102.

Bleam, W. F. and Hoffmann, R. (1988) Isomorphous substitution in phyllosilicates as an electronegativity perturbation: Its effect on bonding and charge distribution: *Phys. Chem. Minerals* **15,** 398–408.

Bolt, G. H. (1979) The ionic distribution in the diffuse double layer: in *Soil Chemistry B. Physico-Chemical Models,* G. H. Bolt, ed., Elsevier, Amsterdam, 1–25.

Brown, I. D. (1978) Bond valences—A simple structural model for inorganic chemistry: *Chem. Soc. Rev.* **7,** 359–376.

Conard, J., Estrade-Szwarckopf H., Dianoux, A. J., and Poinsignon, C. (1984) Water dynamics in a planar lithium hydrate in the interlayer space of a swelling clay. A neutron scattering study: *J. Phys.* **45,** 1361–1371.

Farmer, V. C. (1978) Water on particle surfaces: in *The Chemistry of Soil Constituents,* D. J. Greenland and M. H. B. Hayes, eds., Wiley, New York, 405–448.

Farmer, V. C. and Russell, J. D. (1971) Interlayer complexes in layer silicates. The structure of water in lamellar ionic solutions: *Trans. Faraday Soc.* **67,** 2737–2749.

Foot, J. D. and Colburn, E. A. (1988) Electrostatic potentials for surfaces of inorganic and molecular crystals: *J. Mol. Graphics* **6,** 93–99.

Fripiat, J. G., Lucas, A. A., André, J. M., and Derouane, E. G. (1977) On the stability of polar surface planes of macroscopic ionic crystals: *Chem. Phys.* **21,** 101–104.

Fripiat, J. J., Kadi-Hanifi, M., Conard, J., and Stone, W. E. E. (1980) NMR study of adsorbed water—III. Molecular orientation and protonic motions in the one-layer of a Li hectorite: in *Magnetic Resonance in Colloid and Interface Science,* J. P. Fraissard and H. A. Resing, eds., Reidel, Boston, 529–535.

Giese, R. F. (1979) Hydroxyl orientations in 2:1 phyllosilicates: in *Clays and Clay Minerals, Proc. 13th Natl. Conf., Madison, Wisconsin, 1964,* W. F. Bradley and S. W. Bailey, eds., Pergamon Press, New York, 105–144.

Giese, R. F. (1984) Electrostatic energy models of micas: *Rev. Mineral.* **13,** 105–144.

Heyes, D. M. and van Swol, F. (1981) The electrostatic potential and field in the surface region of lamina and semi-infinite point charge lattices: *J. Chem. Phys.* **75,** 5051–5058.

Hoffmann, R. (1963) An extended Hückel theory. I. Hydrocarbons: *J. Chem. Phys.* **39,** 1397–1412.

Hoffmann, R. and Lipscomb, W. N. (1962) Theory of poly-

hedral molecules. I. Physical factorizations of the secular equation: *J. Chem. Phys.* **36,** 2179–2189.

Jenkins, H. D. B. and Hartman, P. (1979) A new approach to the calculation of electrostatic energy relations in minerals: The dioctahedral and trioctahedral phyllosilicates: *Philos. Trans. Royal Soc. London Ser. A* **293,** 169–208.

Jenkins, H. D. B. and Hartman, P. (1980) Application of a new approach to the calculation of electrostatic energies of expanded di- and trioctahedral micas: *Phys. Chem. Minerals* **6,** 313–325.

Jenkins, H. D. B. and Hartman, P. (1982) Calculations on a model intercalate containing a single layer of water molecules: A study of potassium vermiculite, $K_{2x}Mg_6(Si_{4-x}Al_x)_2O_{20}(OH)_4$, for $1 \leq \times < 0$: *Philos. Trans. Royal Soc. London Ser. A* **304,** 397–446.

Kittel, C. (1986) *Introduction to Solid State Physics:* 6th ed., Wiley, New York, 646 pp.

Kjellander, R. and Marcelja, S. (1985) Polarization of water between molecular surfaces: A molecular dynamics study: *Chemica Scripta* **25,** 73–80.

Lee, J. J. and Guggenheim, S. (1981) Single crystal x-ray refinement of pyrophyllite-1*Tc*: *Amer. Mineral.* **66,** 350–357.

Lee, W. W. and Choi, S.-I. (1980) Determination of the Madelung potential of ionic crystals with a polar surface by the Ewald method: *J. Chem. Phys.* **72,** 6164–6168.

Low, P. F. (1962) Influence of adsorbed water on exchangeable ion movement: in *Clays and Clay Minerals, Proc. 9th Natl. Conf., West Lafayette, Indiana, 1960,* Ada Swineford, ed., Pergamon Press, New York, 219–228.

Mathieson, A. McL. and Walker, G. F. (1954) Crystal structure of magnesium-vermiculite: *Amer. Mineral.* **39,** 231–255.

McBride, M. B. (1989) Surface chemistry of soil minerals: in *Minerals in Soil Environments:* 2nd ed., J. B. Dixon and S. B. Weed, eds., Soil Science Society of America, Madison, Wisconsin, 35–87.

Odom, I. E. (1984) Smectite clay minerals: Properties and uses: *Philos. Trans. Royal Soc. London Ser. A* **311,** 391–409.

Parry, D. E. (1975) The electrostatic potential in the surface region of an ionic crystal: *Surface Sci.* **49,** 433–440.

Parry, D. E. (1976) Errata: The electrostatic potential in the surface region of an ionic crystal: *Surface Sci.* **54,** 195.

Pauling, L. (1929) The principles determining the structure of complex ionic crystals: *J. Amer. Chem. Soc.* **51,** 1010–1026.

Perdikatsis, B. and Burzlaff, H. (1981) Strukturverfeinerung am Talk $Mg_3[(OH)_2Si_4O_{10}]$: *Z. Kristallogr.* **156,** 177–186.

Prost, R. (1975) Interactions between adsorbed water molecules and the structure of clay minerals: Hydration mechanism of smectites: in *Proc. Int. Clay Conf., Mexico City, 1975,* S. W. Bailey, ed., Applied Publishing, Wilmette, Illinois, 351–359.

Shirozu, H. and Bailey, S. W. (1966) Crystal structure of a two-layer Mg-vermiculite: *Amer. Mineral.* **51,** 1124--1143.

Slade, P. G., Stone, P. A., and Radoslovich, E. W. (1985) Interlayer structures of the two-layer hydrates of Na- and Ca-vermiculites: *Clay & Clay Minerals* **33,** 51–61.

Smith, E. R. (1983) Electrostatic potential at a plane surface of a point ionic crystal: *Physica* **120A,** 327–338.

Sposito, G. (1984) *The Surface Chemistry of Soils,* Oxford University Press, New York, 234 pp.

Sposito, G. (1989) Surface reactions in natural aqueous colloidal systems: *Chimia* **43,** 169–176.

Sposito, G. and Prost, R. (1982) Structure of adsorbed water on smectites: *Chem. Rev.* **82,** 553–573.

Veitch, L. G. and Radoslovich, E. W. (1963) The cell dimensions and symmetry of layer-lattice silicates. III. Octahedral ordering: *Amer. Mineral.* **48,** 62–75.

Watson, R. E., Davenport, J. W., Perlman, M. L., and Sham, T. K. (1981) Madelung effects at crystal surfaces: Implications for photoemission: *Phys. Rev. B* **24,** 1791–1797.

Weiss, Z., Rieder, M., Chmielova, M., and Krajicek, J. (1985) Geometry of the octahedral coordination in micas: A review of refined structures: *Amer. Mineral.* **70,** 747–757.

Whangbo, M.-H., Hoffmann, R., and Woodward, R. B. (1979) Conjugated one and two dimensional polymers: *Proc. Royal Soc. London Ser. A* **366,** 23–46.

(Received 24 January 1990; accepted 6 June 1990; Ms. 1979)